Nuclear Engineering and Technology 55 (2023) 1097–1104

Contents lists available at ScienceDirect

Nuclear Engineering and Technology

journal homepage: www.elsevier.com/locate/net

Original Article

Criticality analysis of pyrochemical reprocessing apparatuses for mixed uranium-plutonium nitride spent nuclear fuel using the MCU-FR and MCNP program codes

P.A. Kizub [a, *], A.I. Blokhin [a], P.A. Blokhin [a], E.F. Mitenkova [a], N.A. Mosunova [a], V.A. Kovrov [b], A.V. Shishkin [b], Yu.P. Zaikov [b, c], O.R. Rakhmanova [b, c]

[a] Nuclear Safety Institute, Russian Academy of Sciences, B. Tulskaya Str. 52, Moscow, 115191, Russia
[b] Institute of High-Temperature Electrochemistry, Ural Branch, Russian Academy of Sciences, Akademicheskaya Str. 20, Yekaterinburg, 620990, Russia
[c] Ural Federal University Named After the First President of Russia B.N. Yeltsin, Mira Str., 19, Yekaterinburg, 620002, Russia

ARTICLE INFO

Article history:
Received 3 March 2022
Received in revised form
13 October 2022
Accepted 26 November 2022
Available online 1 December 2022

Keywords:
Spent nuclear fuel
Pyrochemical reprocessing
Pyrochemical apparatuses
Criticality analysis
MCNP
MCU
Effective neutron multiplication factor

ABSTRACT

A preliminary criticality analysis for novel pyrochemical apparatuses for the reprocessing of mixed uranium-plutonium nitride spent nuclear fuel from the BREST-OD-300 reactor was performed. High-temperature processing apparatuses, "metallization" electrolyzer, refinery remelting apparatus, refining electrolyzer, and "soft" chlorination apparatus are considered in this work. Computational models of apparatuses for two neutron radiation transport codes (MCU-FR and MCNP) were developed and calculations for criticality were completed using the Monte Carlo method.

The criticality analysis was performed for different loads of fissile material into the apparatuses including overloading conditions. Various emergency situations were considered, in particular, those associated with water ingress into the chamber of the refinery remelting apparatus. It was revealed that for all the considered computational models nuclear safety rules are satisfied.

1. Introduction

Since the 1950s, hundreds of nuclear reactors have produced 400 000 metric tons of spent nuclear fuel (SNF) [1]. Efficient SNF management is an essential component of an economically viable, safe and proliferation-resistant nuclear fuel cycle solution. One can find a number of the SNF processing technologies ("PUREX", hydrometallurgical, pyrochemical, plasma-chemical, gas-fluoride, etc.). Currently, pyrochemical reprocessing is of wide international interest, since it requires less equipment, makes it possible to reprocess SNF already in the first year after it is unloaded from the reactor, and also contributes to the nonproliferation of nuclear materials [2]. Research and development of this technology is being carried out in Russia [3–9], the United States of America [10,11], the Republic of Korea [12,13], Japan [14], India [15] and Europe [16].

In Russia, a combined technology, including principal, pyrochemical and hydrometallurgical conversions, is considered as the basic option for the reprocessing mixed uranium-plutonium nitride (MNUP) SNF from the BREST-OD-300 reactor in the reprocessing module of the experimental demonstration energy complex (RMEDEC) [8]. The technology is already evaluated on laboratory scale equipment and demonstration complex design is currently under development. The simplified reprocessing technology diagram is presented in Fig. 1.

Previous criticality analysis of similar-scale apparatuses uses very simplified models: SNF and metal components are represented as two coaxial cylinders [13]. But real pyrochemical apparatuses participating in the technological chain of the SNF reprocessing are complex heterogeneous systems and in order to assess their k_{eff} precisely detailed models and certified, verified and validated neutron radiation transport codes are required.

This study is devoted to a preliminary criticality analysis of novel, in terms of configuration and technology, pyrochemical apparatuses, which include high-temperature treatment apparatuses, a "metallization" electrolyzer, refinery remelting apparatus, refining electrolyser, and "soft" chlorination apparatus of the

* Corresponding author.
E-mail address: kizub@ibrae.ac.ru (P.A. Kizub).

https://doi.org/10.1016/j.net.2022.11.020

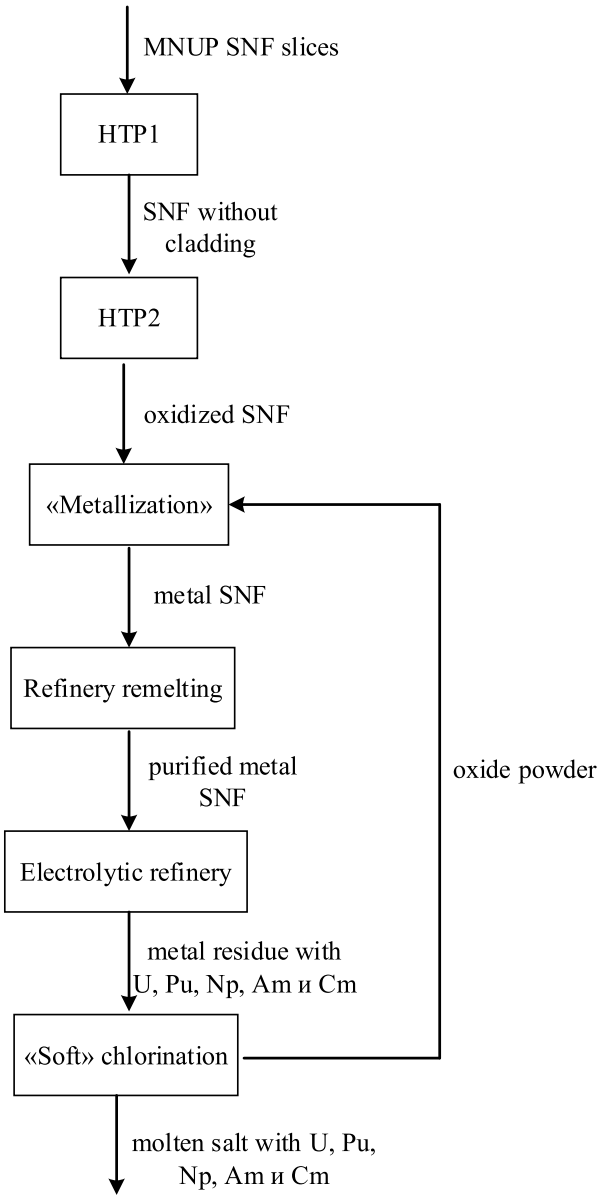

Fig. 1. MNUP SNF pyrochemical reprocessing diagram.

RMEDEC. The criticality analysis is carried out for regular operation loads of fissile material (FM) into the apparatus and for overloading conditions, i.e. with an increased mass of the FM (such a scenario may be caused by a failure of the program of the robot that is loading the FM). In addition, other violations of regular operation are considered, for example, cooling the installations and forming the FM spillages in the "metallization" apparatus. For the refining remelting devices, considering the presence of water cooling of the chamber shell, the installation is analyzed for emergency scenarios associated with the ingress of water into the chamber and crucible.

2. Calculation method

Main way to perform criticality analysis is to compute the effective neutron multiplication factor k_{eff}. Russian Nuclear Safety Rules for Nuclear Fuel Cycle Facilities NP-063-05 [17] states that the facility is safe if k_{eff} <0.95 during regular operation, and k_{eff} <0.98 during violations of regular operation. The Monte Carlo Universal (MCU-FR) [18] and Monte Carlo N-Particle Transport Code (MCNP) [19] program codes, which are based on the Monte Carlo method, were used to calculate k_{eff} for each of the model apparatuses. The MCU family codes was developed at the National Research Center "Kurchatov Institute" to perform calculations of WWERs. Currently it is used in Russia Federation in solving fission reactors and radiation protection issues [20]. The MCNP family codes are a kind of standard and are widely used in the world's leading laboratories in the USA and Europe in international benchmarks. The calculations using the MCNP codes confirm the reliability of the results obtained, therefore, for each device, a comparative analysis of k_{eff} values according to the MCU-FR and MCNP codes was performed.

The estimated nuclear data based on the JEFF-3.3 library [21] were used in the MCNP calculations. In the MCU-FR calculations, built-in estimated neutron data from ROSFOND [22] in the "ace" format were used (using MDBFR60 block).

3. Description of the calculation models of the apparatuses

Fragments of fuel elements of the MNUP SNF from the central zone of the BREST-OD-300 reactor with a burnup of 80 MWd/kgHM (with initial enrichment 13.5% [23]) after one year of exposure in a temporary storage facility (TSF) and 0.5 year of exposure outside the TSF were sent to the RMEDEC for the reprocessing. The technological chain of RMEDEC pyrochemical procedure is represented as a sequence of installations: 1)-2) devices for high-temperature processing No. 1 and 2; 3) "metallization" apparatus (electrolyzer); 4) apparatus for refining remelting; 5) apparatus for electrolytic refining; 6) apparatus for "soft" chlorination [7–9]. The MCNP and MCU-FR criticality calculations were performed for these six devices.

3.1. High-temperature processing apparatus

High-temperature processing apparatuses No.1 and 2 (HTP1 and HTP2) are basic pyrochemical devices designed to remove the light fission products from fuel element fragments of the MNUP SNF supplied for pyrochemical processing. HTP1 is a vertical retort (reactor) integrated into a high-temperature electric resistance furnace (the furnace is not included in the design model). The incoming product is loaded into a retort. In the end cover of the retort, there are gas ducts (not included in the design model) for purging the internal bulk of the reactor. The gas captures and removes the formed light fission products (FP) from the apparatus.

Calculations for the criticality of the HTP1 were carried out for two operating scenarios: "Loading" and "De-nitration". The geometry of the device model for these scenarios is schematically shown in the projection of the section along the *Oz* axis in Fig. 2. For each operating mode of the HTP1, the assumed SNF loading with a mass of 30 kg and an increased SNF loading with a mass of 50 kg are considered. The SNF powder supplying for reprocessing in the HTP1 has a porosity of 60% and is modeled as a homogeneous medium, in which 60% by volume is gas, and the remaining 40% is the MNUP SNF with a bulk density of 6.6 g/cm^3.

The apparatus of HTP2 is also a vertical retort integrated into a high-temperature furnace (the furnace is not included in the design model). The initial product is a powder coming from operation HTP1. It is loaded for processing into a retort. In the end cover of the retort, there are gas ducts (not included in the design model) for purging the internal volume of the reactor with a gas.

Calculations for the criticality of the HTP2 were carried out for three operating scenarios: "Loading", "Oxidation" and "Distillation". The geometry of the apparatus model for these scenarios is also schematically shown in the projection along the *Oz* axis in

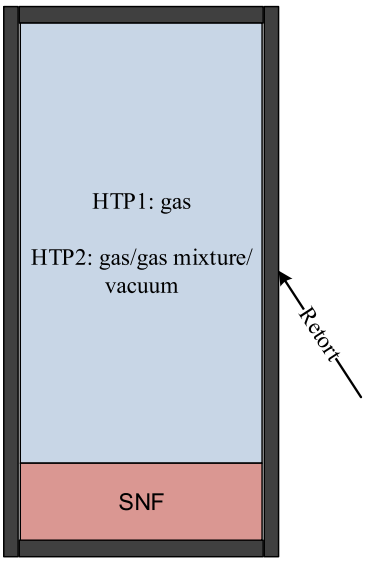

Fig. 2. Schematic image of high-temperature processing apparatuses No. 1 and 2 in the projection along the *Oz* axis.

Fig. 2. "Loading" with filling the retort with gas, "Oxidation" with filling the retort with a gas mixture and "Distillation" with vacuum filling. The gas/gas mixture/vacuum volumes depend on the mass of the MNUP SNF loaded into the retort. For each operating mode of the HTP2, the design SNF loading with a mass of 31 kg and an increased SNF loading with a mass of 52 kg are considered. Increased loading compared to HTP1 is caused by presence of SNF dust on the retort walls. The SNF powder supplied for reprocessing in the HTP2 has a porosity of 60% and is modeled as a homogeneous medium, in which 60% by volume is gas/gas mixture/vacuum, and the remaining 40% is the SNF without cladding with a bulk density of 5.6 g/cm^3.

3.2. "Metallization" apparatus

The "metallization" apparatus is a basic pyrochemical apparatus (electrolyzer) designed for the electrochemical reduction of the target components (U, Pu, Np, Am and Cm) of the SNF to metal. For pyrochemical processing this apparatus receives SNF, which undergone compaction (granulation) and oxidation as a result of high-temperature processing operations. The operating temperature of the "metallization" electrolyzer is ~900 K. In the course of the "metallization" process the following procedures are carried out: reduction of oxides of U, Pu, Np, Am, Cm to metals; removal of gaseous oxide reduction products, i.e., oxygen is removed from the operating space of the electrolyzer using an inert gas (Ar) flow; removal from the flow of target components a part of the fission products, i.e., alkali and alkaline earth metals in the form of chlorides dissolved in the electrolyte.

A schematic image of the simplified model of an electrolyzer (section along the *Oz* axis) and a top view are shown in Fig. 3. A vertical retort is integrated into the high-temperature furnace (the furnace is not included in the design model), on the bottom of which a crucible with an electrolyte (LiCl - Li_2O melt) is installed. The cathode unit includes a cathode, a basket and a current lead. The basket has a cylindrical shape and is used to load the initial product - granules of the oxidized SNF. The basket is filled with granules 90-95%. The anode unit includes a ceramic gas duct, a ceramic anode and a current lead.

The process of gaseous oxygen release occurs due to the oxidation of oxide anions from the melt. The released oxygen is localized and removed from the apparatus with a carrier gas flow (dry argon). The argon is fed into the common space of the electrolyzer, and the removal of the Ar + O_2 gas mixture occurs through the anode units with the gas outlet from the apparatus through the upper part of the gas ducts.

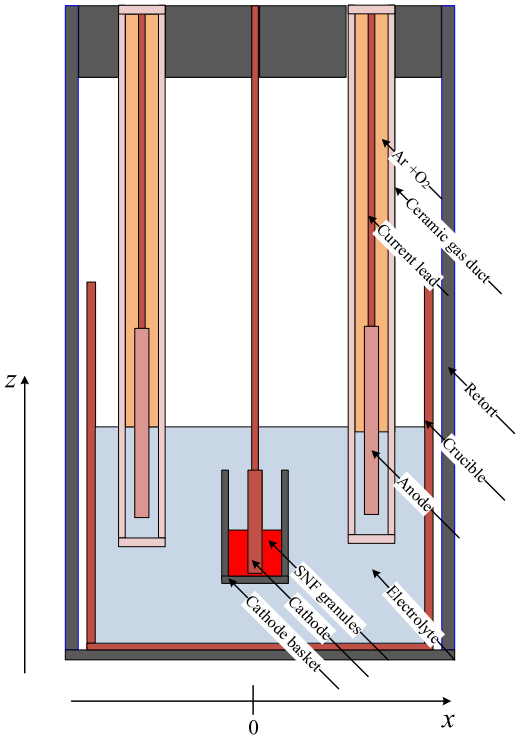

a) section along the *Oz* axis

Fig. 3a. Schematic image of the "metallization" apparatus
a) section along the Oz axis.

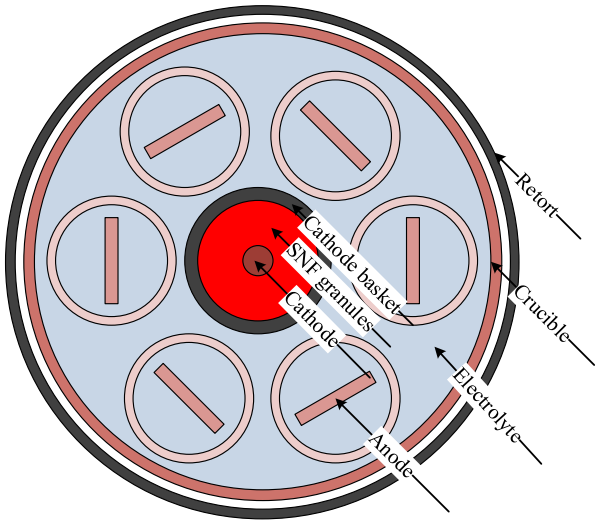

b) top view

Fig. 3b. Schematic image of the "metallization" apparatus
b) top view.

The SNF granules have a porosity of 40% and are modeled as a homogeneous medium, in which 40% by volume is electrolyte, and the remaining 60% are the SNF granules with a bulk density of 2.7 g/cm^3.

The k_{eff} calculation is carried out for various scenarios of the "metallization" apparatus operation which are defined by its mechanical design. The apparatus has a perforated cathode basket; therefore, various cases of spillage of the SNF granules on the bottom of the crucible are investigated. Three variants of spillage are studied: height H = 10, 20 and 30 cm (maximum possible spillage to the level of the cathode basket). A case of spillage H = 30 cm was also investigated with an increased electrolyte level by 16 cm (due to the possibility of its displacement by the spillage).

The models used in the variant calculations of k_{eff} of the "metallization" apparatus are listed in Table 1.

Spillage of the SNF granules at the bottom of the crucible of the the "metallization" apparatus (especially for the H = 10 cm variant) can lead to the production of a weakly coupled system [24], since two remote zones with FP are formed. The weakly coupled systems are characterized by slow convergence of the calculated functionals, which leads to the need for analyzing the stability and correctness of fission neutron sources (sets of points at which neutrons were produced) to check the reliability of the results obtained.

In this regard, in the calculations using the MCNP code, the distributions of fission sources along the *Ox* axis were obtained and analyzed for the "metallization" apparatus when the cathode basket is completely filled with the SNF granules and in the presence of a spillage with a level of H = 0, 10, 20, and 30 cm. The fission sources for the "metallization" apparatus with 16.1 million neutron histories are given in Fig. 4. The initial distribution of sources was set to be homogeneously distributed over the entire volume of the SNF in the cathode basket and at the bottom of the crucible. The

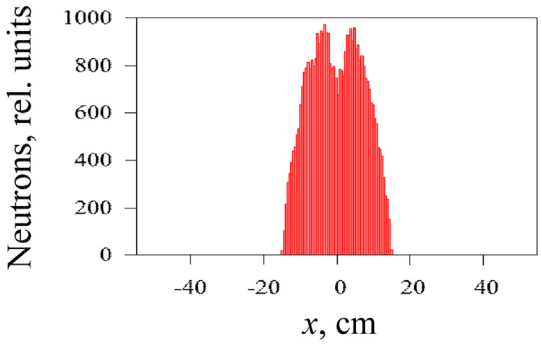

Fig. 4a. Distribution of the fission neutron source along the *Ox* axis for the "metallization" apparatus with a) maximum loading the cathode basket and with a spillage.

Table 1
Calculated values of the neutron multiplication coefficient k_{eff} for all computational models of apparatus.

Operation scenario of apparatus	k_{eff} ± 0.0001		$(k_{eff\_MCNP}-k_{eff\_MCU})/k_{eff\_MCNP}$, %
	MCU	MCNP	
Apparatus HTP1, T_{calc} = 300/1500 K (depending on the operating mode)			
«Loading», M_{SNF} = 30 kg	0.1096	0.1089	0.6
«Loading», M_{SNF} = 50 kg	0.1556	0.1547	0.6
«De-nitration», M_{SNF} = 30 kg	0.1096	0.1089	0.7
«De-nitration», M_{SNF} = 50 kg	0.1558	0.1548	0.7
Apparatus HTP2, T_{calc} = 300/1200 K (depending on the operating mode)			
«Loading», M_{SNF} = 31 kg	0.1131	0.1122	0.7
«Loading», M_{SNF} = 52 kg	0.1585	0.1573	0.8
«Oxidation», M_{SNF} = 31 kg	0.1130	0.1122	0.7
«Oxidation», M_{SNF} = 52 kg	0.1585	0.1572	0.8
«Distillation», M_{SNF} = 31 kg	0.1134	0.1123	1
«Distillation», M_{SNF} = 52 kg	0.1585	0.1573	0.8
"Metallization" apparatus, T_{calc} = 900 K			
M_{SNF} = 30 kg	0.1271	0.1263	0.6
M_{SNF} = 53.76 kg without spillage	0.1575	0.1567	0.5
With spillage H = 10 cm	0.1690	0.1688	0.1
With spillage H = 20 cm	0.2514	0.2511	0.1
With spillage H = 30 cm	0.3239	0.3240	0.1
With spillage H = 30 cm, T_{calc} = 300 K	0.3238	0.3241	0.1
With spillage H = 30 cm, electrolyte level + 16 cm	0.3261	0.3264	0.1
Refinery remelting apparatus, T_{calc} = 1800 K			
M_{SNF} = 50 kg in the shape of a cylinder	0.4881	0.4686	4.2
M_{SNF} = 90 kg in the shape of a ball	0.6356	0.6293	1
M_{SNF} = 90 kg, water in crucible	0.6769	0.7174	5.6
M_{SNF} = 90 kg, water in chamber	0.7068	0.7106	0.5
M_{SNF} = 90 kg, water in crucible and chamber	0.7395	0.7549	2
Electrolytic refinery apparatus, T_{calc} = 900 K			
M_{SNF} = 47 kg in the shape of a cylinder	0.4297	0.4253	1
M_{SNF} = 90 kg in the shape of a ball	0.6337	0.6278	0.9
"Soft" chlorination apparatus, T_{calc} = 900 K			
P_{SNF} = 90%, M_{SNF} = 5 kg	0.0566	0.0561	0.8
P_{SNF} = 50%, M_{SNF} = 25 kg	0.2573	0.2551	0.9
P_{SNF} = 30%, M_{SNF} = 35 kg	0.3477	0.3444	1
P_{SNF} = 30%, M_{SNF} = 45 kg	0.3636	0.3579	1.6

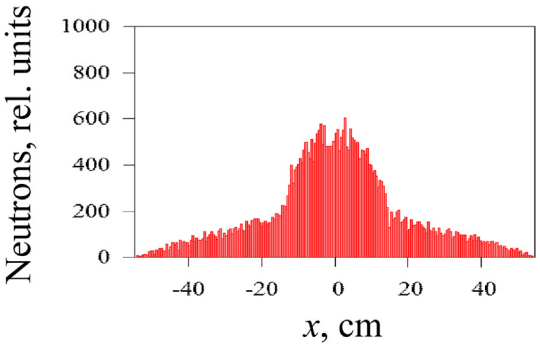

Fig. 4b. Distribution of the fission neutron source along the *Ox* axis for the "metallization" apparatus with a) maximum loading the cathode basket and with a spillage and with a spillage at the bottom of the crucible with a height of 10 cm b).

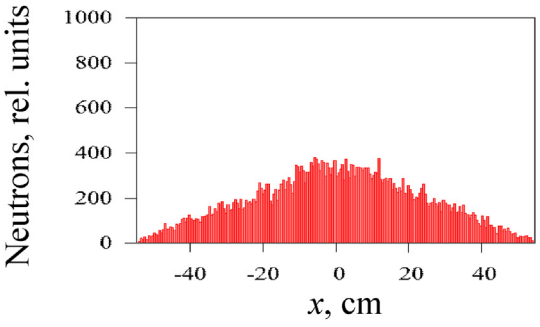

Fig. 4c. Distribution of the fission neutron source along the *Ox* axis for the "metallization" apparatus with a) maximum loading the cathode basket and with a spillage and with a spillage at the bottom of the crucible with a height of 20 cm c).

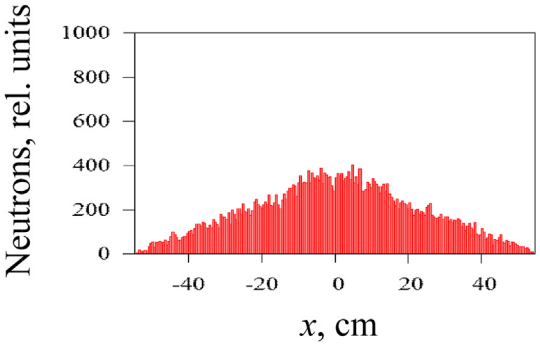

Fig. 4d. Distribution of the fission neutron source along the *Ox* axis for the "metallization" apparatus with a) maximum loading the cathode basket and with a spillage and with a spillage at the bottom of the crucible with a height of 30 cm d).

methodology for representing the fission source is described in [24,25].

The obtained distributions of fission neutrons (Fig. 4) have a symmetric form and do not contradict the distribution of FP in the system: both zones with FP act as neutron sources. Moreover, even in the case of maximum spillage ($H = 30$ cm), the largest contribution to the source is made by the SNF granules located in the cathode basket of the apparatus. The "dip" in the distribution in the region corresponding to the central part of the basket is associated with the presence of a cathode current lead here.

Thus, the analysis of fission sources revealed that the "metallization" apparatus is not a weakly coupled system that requires additional analysis of the convergence of the calculated functionals. It can also be concluded that the maximum contribution to k_{eff} is made by the FP located in the basket, despite the significantly lower mass compared to the FM located at the bottom of the crucible.

3.3. Refinery remelting apparatus

The refinery remelting apparatus is a basic pyrochemical apparatus designed to produce a metal alloy based on the target components of the MNUP SNF reprocessing (U, Pu, Np, Am and Cm) and "noble" FP (Pd and Ag). The device also removes the target components of the main part of the rare earth elements and Zr (FP) in the form of oxides.

A schematic image of the simplified geometry for the model of the refinery remelting apparatus in the projection along the *Oz* axis is presented in Fig. 5. The apparatus is an induction furnace with an inductor placed in a sealed chamber to create an inert atmosphere (argon). The camera body has a cylindrical shape and consists of two shells. Water is supplied to the space between the shells to cool the body. In an inductor located in the central part of the chamber a crucible made of BeO with initial products is placed on a concrete support. The crucible is covered with a lid. The working temperature of the device is 1800 K. The apparatus is designed to allow maximum density of the initial product (metal alloy) of 19.2 g/cm^3.

The calculation of k_{eff} of the refinery remelting apparatus was carried out for a normal load, $M_{SNF} = 50$ kg (16% of the crucible volume), when the target product has the shape of a cylinder, and for an increased load, $M_{SNF} = 90$ kg, when the target product is a ball with a shell of BeO.

The highest k_{eff} is reached in a situation when a facility with FM is flooding with water, which in this case plays the role of a neutron moderator. As mentioned above, water is supplied to the refinery remelting apparatus for cooling (in the space between the shells of the casing), therefore, various scenarios of emergency flooding the installation were considered for this apparatus:

- a hole in the inner shell of the chamber, water enters the crucible: $M_{SNF} = 90$ kg, target product in the form of a ball with a shell of BeO, water in the crucible (Fig. 6a), 300 K;
- a hole in the inner shell of the chamber, water enters the chamber: $M_{SNF} = 90$ kg, target product in the form of a ball with a shell of BeO, water in the chamber (Fig. 6b), 300 K;

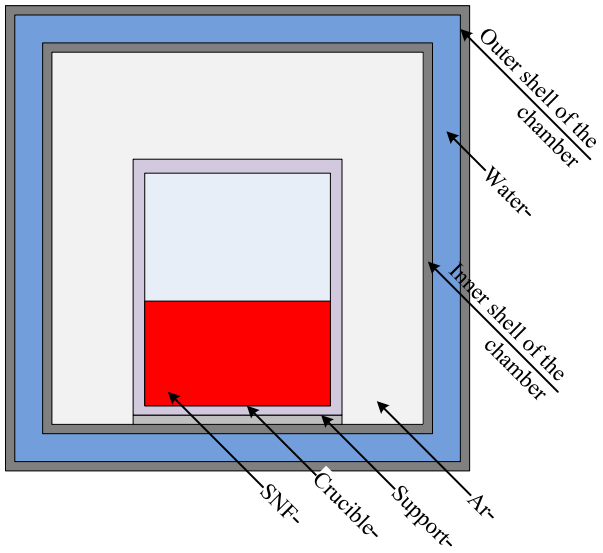

Fig. 5. Schematic image of the refinery remelting apparatus (projection along the *Oz* axis).

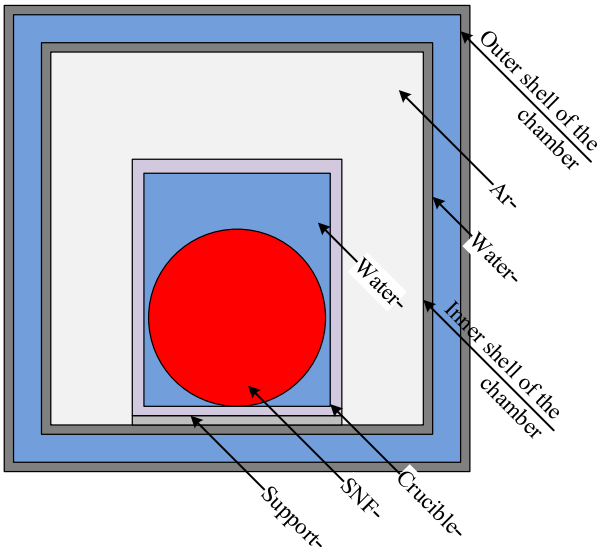

a) - water enters the crucible

Fig. 6a. Various options for flooding the refinery remelting apparatus
a) - water enters the crucible.

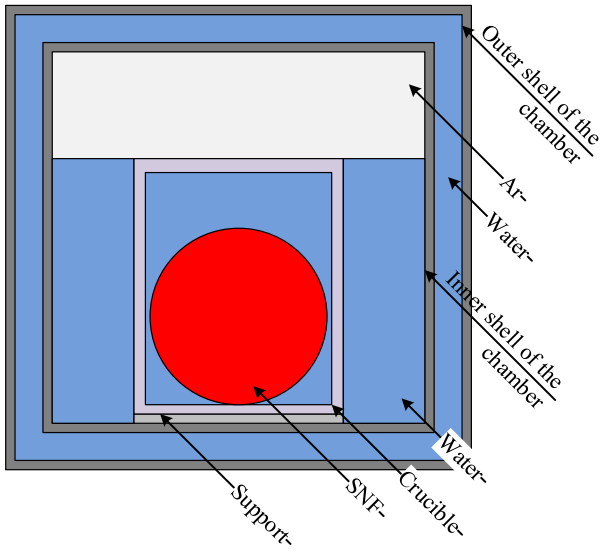

c) - water enters the crucible and chamber

Fig. 6c. Various options for flooding the refinery remelting apparatus
c) - water enters the crucible and chamber.

– a hole in the inner shell of the chamber, water enters the crucible and the chamber: $M_{SNF} = 90$ kg, the target product in the form of a ball with a shell of BeO, water in the crucible and chamber (Fig. 6c), 300 K.

The models used in the criticality calculations for the refinery remelting apparatus are listed in Table 1.

3.4. Electrolytic refinery apparatus

An electrolytic refinery apparatus is a basic pyrochemical apparatus designed to purify target components (U, Pu, Np, Am, and Cm) of the SNF from fission products, i.e., fractions of "noble" FP. A metal alloy based on target components, obtained after refining remelting, is fed to the electrolyzer for pyrochemical processing.

A schematic image of the simplified geometry of the refining cell model (projection along the *Oz* axis) is shown in Fig. 7. The electrolyzer is a vertical retort integrated into a high-temperature furnace (not included in the model). The retort provides sealing of the working space of electrolyzer and carrying out electrorefining at ~800 K in an inert atmosphere of high-purity argon. The retort lid is used to accommodate and enter into the working space of the retort anode and cathode current leads (not included in the design model).

Calculation of k_{eff} of the refining electrolyzer is given for normal operating conditions, i.e., $M_{SNF} = 47$ kg and the target product has the shape of a cylinder, as well as for increased loading of fission

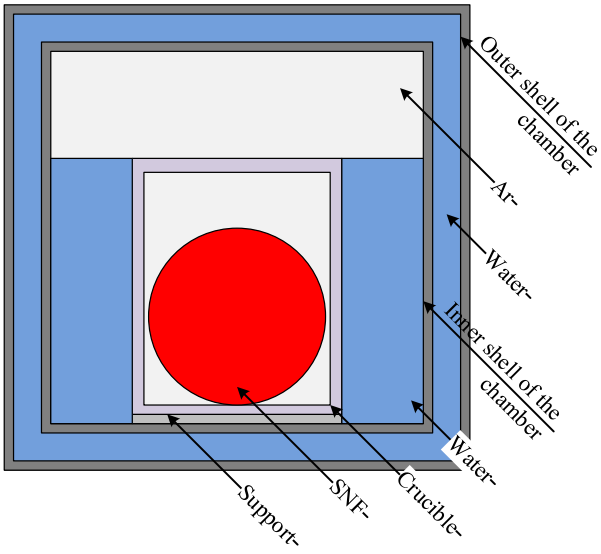

b) - water enters the chamber;

Fig. 6b. Various options for flooding the refinery remelting apparatus
b) - water enters the chamber.

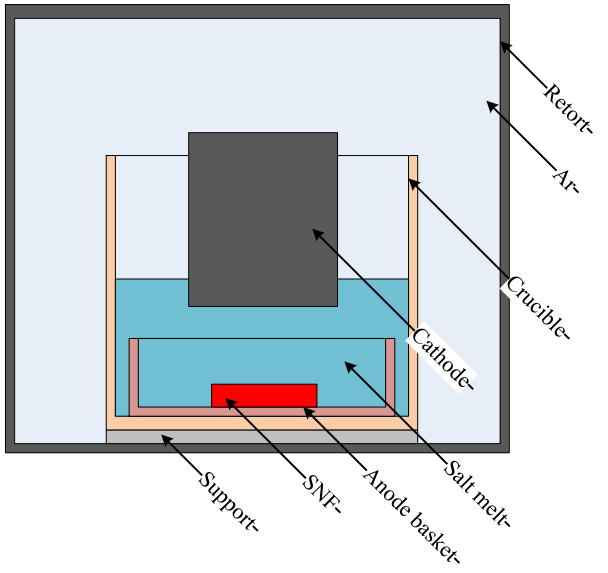

Fig. 7. Schematic image of an electrolytic refinery apparatus along the *Oz* axis.

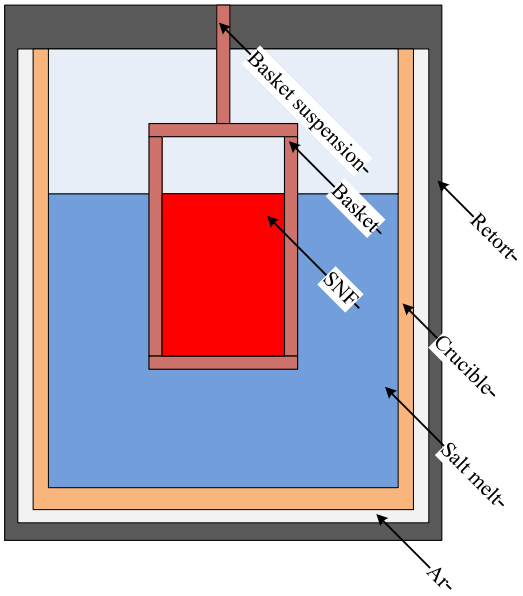

Fig. 8. Schematic image of the "soft" chlorination apparatus.

products, i.e. $M_{SNF} = 90$ kg and the target product is in the shape of the ball.

3.5. "Soft" chlorination apparatus

The "soft" chlorination apparatus is a basic pyrochemical apparatus designed to dissolve in the form of chlorides the target components of the SNF reprocessing (U, Pu, Np, Am, and Cm) contained in the anode deposit. The apparatus receives the "anode deposit" for pyrochemical processing after the electrolytic refining. SNF is a porous metal alloy of "noble" FP and target components. The initial product of the "soft" chlorination operation has a porosity of 90% vol. and a bulk density of 1.9 g/cm^3.

A schematic image of the "soft" chlorination apparatus model (projection along the *Oz* axis) is shown in Fig. 8. The apparatus is integrated into a resistance furnace (the furnace is not included in the model) and in a steel retort, in which a crucible with chloride melt is placed. In the lid of the retort, a basket is fixed with a suspension, into which the original product for processing is loaded. The mass of the initial product is 5 kg, which occupies the inner volume of the basket by 80%. The operating temperature of the apparatus is 800–900 K.

The calculation of k_{eff} was carried out for various operation scenarios of the "soft" chlorination apparatus. The considered models are listed in Table 1 and differ in the setting of the porosity of the SNF (P_{SNF}) and, as a consequence, the M_{SNF}.

4. Calculation results

The calculated values of the neutron multiplication coefficients k_{eff} for all model apparatuses are given in Table 1. For HTP1 and HTP2 k_{eff} is determined to a great extent by the SNF mass, and not by the composition of the gas mixture inside the retort. An increase in the mass of the single SNF load in this case by a factor of 1.7 leads to a rise in the k_{eff} value by the factor of 1.4. According to the safety rules, such an increase in the SNF loading is allowed for HTP1 and HTP2 ($k_{eff} < 0.95$).

For the "metallization" apparatus the maximum possible spillage (30 cm) of the SNF granules leads to a twofold increase in k_{eff}. The operating temperature of the apparatus has no significant effect on k_{eff}. An increase in the electrolyte level in the crucible due to its displacement by the SNF granules spillage results in the rise in the k_{eff} value by less than 1%. According to the safety rules, an increase of the SNF loading by a factor of 1.7 for the "metallization" apparatus is allowed, even in cases of granules spillage on the bottom of the crucible ($k_{eff} < 0.95$).

For a refinery remelting apparatus, an increase of the SNF load mass by a factor of 1.8 leads to an increase in k_{eff} by a factor of 1.3. The spherical shape of the target product in a shell of beryllium oxide does not lead to $k_{eff} = 0.95$. The "safest" scenario for flooding the refinery remelting apparatus is an emergency when water only enters the crucible; in this case, k_{eff} increases by a factor of 1.1. The most "dangerous" scenario for the flooding of the refining remelting apparatus is an emergency when water is in both the crucible and the chamber, in which case k_{eff} increases by 1.2 times. According to the safety rules, the increase in the SNF loading for a refinery remelting apparatus is allowed ($k_{eff} < 0.95$).

For the electrolytic refinery apparatus, an increase of SNF load mass by a factor of 1.9 leads to an increase in the k_{eff} value by a factor of 1.5; the spherical shape of the target product does not lead to $k_{eff} = 0.95$. According to the safety rules, the increase in the SNF loading for the electrolytic refinery apparatus is allowed ($k_{eff} < 0.95$).

For the "soft" chlorination apparatus, the five-fold increase in the mass of the single SNF loading leads to an increase in the k_{eff} value by a factor of 4.5. A seven-fold increase in the mass of the single SNF load leads to the 6-fold increase in the k_{eff} value. An increase in the mass of the single SNF load by a factor of 9 leads to the rise in the k_{eff} value by a factor of 6.5. According to the safety rules, an increase in the SNF load by the factor of 9 for an electrolytic refinery apparatus is allowed ($k_{eff} < 0.95$).

Comparison of the calculation results obtained using the MCU-FR code with the results obtained using the MCNP standard code make it possible to conclude that for electrolytic refining, the "metallization", HTP1and HTP2, the differences in k_{eff} are less than 1%; for the refinery remelting apparatus, the difference k_{eff} is 6%; for the apparatus of "soft" chlorination, the difference k_{eff} is less than 2%. The obtained differences of k_{eff} may be due to the use of different nuclear databases.

It should be noted that MCNP calculations were performed with different pseudorandom seed to control calculation convergence. This is configured using *dbcn* card [19]. Calculation results give the same k_{eff} for different pseudorandom seed, which indicates that it is correct.

For "metallization" apparatus with spillage $H = 30$ cm two additional calculations with simplified geometry were performed: with Godiva-like and cylindrical geometry. SNF and metal mass are preserved the same. Following results were obtained:

- $k_{eff} = 0.59$ for Godiva-like geometry;
- $k_{eff} = 0.47$ for cylindrical geometry.

Comparing this to $k_{eff} = 0.32$ for detailed model (see Table 1) one can see that k_{eff} is overestimated for simplified models.

5. Conclusions

Within the existing technological scheme of pyrochemical processing of the RMEDEC for the reprocessing the MNUP SNF of the BREST-OD-300 reactor, a criticality analysis of novel pyrochemical apparatuses was performed: high-temperature processing apparatus, the "metallization" apparatus, the refinery remelting apparatus, the refining electrolyzer and the "soft" chlorination apparatus. For this purpose, computational models were developed

for all apparatuses using the MNUP SNF loading rate and increased loading. Calculations for criticality were performed using the Monte Carlo method via the MCU-FR and MCNP codes. Based on criticality analysis, the following conclusions were made:

1) all the considered apparatuses are safe both during regular operation using the rate of loading of fissile materials, and when deviating from the conditions of regular operation, i.e., with a possible increase in the mass of a single load of fissile materials by a factor of 1.6;
2) the "metallization" apparatus is safe in the presence of significant spillages of the spent nuclear fuel granules (up to the level of the cathode basket);
3) the most significant data related to k_{eff} were obtained for the refinery remelting apparatus in the version of the model with an increased load and the presence of water in the apparatus;
4) the "soft" chlorination apparatus is safe if it deviates from the conditions of normal operation, i.e., with a possible increase in the mass of a single charge of fissile materials by nine times.

For all the considered computational models of the SNF pyrochemical reprocessing apparatuses the neutron multiplication factor $k_{eff} < 0.95$.

In continuation of our work, we suggest to expand the study of the "metallization" apparatus regarding nuclear weapons to consider emergency scenarios, for example, those associated with flooding; to study the dynamic distribution of the SNF during electrolysis, when the SNF has the composition of the target product (final composition) and intermediate composition; consider the inhomogeneous spillage of the spent nuclear fuel pellets at the bottom of the crucible and analyze the looseness of such a system.

Declaration of competing interest

The authors declare that they have no known competing financial interests or personal relationships that could have appeared to influence the work reported in this paper.

Appendix A. Supplementary data

Supplementary data to this article can be found online at https://doi.org/10.1016/j.net.2022.11.020.

References

[1] Nuclear Technology Review 2020, International Atomic Energy Agency, 2020, pp. 1–67. GC(64)/INF/2.
[2] R.G. Lewin, M.T. Harisson, International developments in electrorefining technologies for pyrochemical processing of spent nuclear fuels, in: Robin Taylor, Reprocessing and Recycling of Spent Nuclear Fuel, first ed., Woodhead Publishing, 2015, pp. 373–413.
[3] A. Salyulev, A. Potapov, V. Khokhlov, V. Shishkin, The electrical conductivity of model melts based on LiCl-KCl, used for the processing of spent nuclear fuel, J. Electrochim. Acta 257 (2017) 510–515.
[4] A. Zhitkov, A. Potapov, K. Karimov, V. Shishkin, A. Dedyukhin, Y. Zaykov, Interaction between UN and $CdCl_2$ in molten LiCl-KCl eutectic. I. Experiment at 773 K, J. Nucl. Eng. Technol. 52 (2020) 123–134, https://doi.org/10.1016/j.net.2019.07.006.
[5] A. Salyulev, A. Potapov, Electrical conductivity of $(LiCl–KCl)_{eut.}–SrCl_2$ molten mixtures, J. Chem. Eng. Data 66 (12) (2021) 4563–4571, https://doi.org/10.1021/acs.jced.1c00591.
[6] A.B. Salyulev, A.V. Shishkin, V. Yu. Shishkin, Yu.P. Zaikov, Distillation of lithium chloride from the products of uranium dioxide metallization, J. At. Energy 126 (4) (2019) 226–229, https://doi.org/10.1007/s10512-019-00541-1.
[7] Yu.P. Zaikov, V. Yu. Shishkin, A.M. Potapov, A.E. Dedyukhin, V.A. Kovrov, A.S. Kholkina, V.A. Volkovich, I.B. Polovov, Research and Development of the pyrochemical processing for the mixed nitride uranium-plutonium fuel, J. Phys. Conf. Ser. 1475 (2020), 012027, https://doi.org/10.1088/1742-6596/1475/1/012027.
[8] E.O. Adamov, Yu.S. Mochalov, V.I. Rachkov, Yu.S. Khomyakov, A. Yu. Shadrin, V.A. Kascheev, A.V. Khaperskaya, Spent nuclear fuel reprocessing and nuclear materials recycling in two-component nuclear energy, J. At. Energy 130 (1) (2021) 29–35, https://doi.org/10.1088/1742-6596/1475/1/012027.
[9] A.A. Zherebtsov, Yu.S. Mochalov, A.Yu. Shadrin, Yu.P. Zaikov, M.K. Gorbachev, K.A. Sokolov, V.A. Kisly, D.A. Goncharov, Development of the general design of the industrial energy complex with CNFC, J. Phys. Conf. Ser. 1475 (2020), 012007, https://doi.org/10.1088/1742-6596/1475/1/012007.
[10] J.J. Laidler, et al., Development of pyroprocessing technology, J. Prog. Nucl. Energy 31 (1) (1997) 131–140.
[11] M.F. Simpson, Developments of Spent Nuclear Fuel Pyroprocessing Technology at Idaho National Laboratory, Idaho National Laboratory, 2012, pp. 1–21. INL/EXT-12-25124.
[12] J.-G. Kim, S.-J. Lee, S.-B. Park, S.-C. Hwang, H. Lee, High-throughput electrorefining system with graphite cathodes and a bucket-type deposit retriever, J. Procedia Chem. 7 (2012) 754–757.
[13] F. GAO, et al., Criticality safety evaluation of materials concerning pyroprocessing, J. Nucl. Sci. Technol. 48 (6) (2011) 919–928.
[14] T. Inoue, T. Koyama, Y. Arai, State of the art of pyroprocessing technology in Japan, J. Energy Procedia. 7 (2011) 405–413.
[15] K. Nagarajan, et al., Development of pyrochemical reprocessing for spent metal fuels, J. Energy Procedia. 7 (2011) 431–436.
[16] E. Mendes, et al., Application of the pyrochemical DOS, developed by the CEA, within reprocessing of CERCER transmutation fuel targets, J. Procedia Chem. 21 (2016) 433–440.
[17] Federal (Russian) Rules and Regulations in the Field of Nuclear Energy Use Nuclear Fuel Cycle Facilities, Federal Environmental, Industrial and Nuclear Supervision Service, 2005, pp. 1–37. NP-063-05 (in Russian).
[18] M.A. Kalugin, D.S. Oleynik, D.A. Shkarovsky, Overview of the MCU Monte Carlo software package, J. Ann. Nucl. Energy 82 (2015) 54–62.
[19] X-5 Monte Carlo Team, MCNP – A General Monte Carlo N-Particle Transport Code, Version 5, Los Alamos National Laboratory, 2008, pp. 1–416. LA-UR-03-1987.
[20] N.I. Alekseev, S.N. Bol'shagin, E.A. Gomin, S.S. Gorodkov, M.I. Gurevich, M.A. Kalugin, A.S. Kulakov, S.V. Marin, A.P. Novosel'tsev, D.S. Oleynik, A.V. Pryanichnikov, E.A. Sukhino-Khomenko, D.A. Shkarovskiy, M.S. Yudkevich, The status of MCU-5, J. Phys. At. Nuclei 75 (14) (2012) 1634–1646.
[21] A. Plompen, et al., The joint evaluated fission and fusion nuclear data library, JEFF-3.3, J. Eur. Phys. J. A 56 (2020) 181. ISSN 1434-6001. JRC118001.
[22] S.V. Zabrodskaya, A.V. Ignatyuk, V.N. Koshcheev, V.N. Manokhin, M.N. Nikolaev, V.G. Pronyaev, ROSFOND – Russian national library of neutron data, J. Problems of atomic science and technology, Ser. Nucl. constants 1 – 2 (2007) 3–21 (in Russian).
[23] A.G. Glazov, V.N. Leonov, V.V. Orlov, A.G. Sila-Novitskii, V.S. Smirnov, A.I. Filin, V.S. Tsikunov, Brest reactor and plant-site nuclear fuel cycle, J. At. Energy 103 (1) (2007) 501–508.
[24] P.A. Kizub, E.F. Mitenkova, Fission Neutron Source in Monte Carlo Calculations for Loosely Coupled Systems, Nuclear Safety Institute of the Russian Academy of Sciences, 2015, pp. 1–30. IBRAE-2015-02 (in Russian).
[25] E.F. Mitenkova, D.A. Koltashev, P.A. Kizub, Distribution of the fission reaction rate in a loosely coupled system for the "checkerboard" test model, J. At. Energy 116 (6) (2014) 345–349.